Electronic structure and properties of superconducting $LiTi_2O_4$

S. Massidda, Jaejun Yu, and A. J. Freeman
Materials Research Center and Department of Physics and Astronomy, Northwestern University, Evanston, Illinois 60208
(Received 27 June 1988)

We present results of precise local-density calculations of the electronic structure for the superconducting spinel oxide $LiTi_2O_4$ as obtained with the full-potential linearized augmented-plane-wave method. Self-consistent calculations are performed for both the observed (distorted) and ideal (undistorted) spinel structures. The results show important changes in the electronic states near E_F between the two structures. Unlike the case of Cu d states in the high-T_c Cu-O superconductors, the Ti d bands are separated by an $\sim$2.6-eV energy gap from the O p bands, and are further split into t_{2g} and e_g bands. The states around E_F have predominant Ti d character, with a substantial hybridization with O p states. Crude rigid-ion calculations indicate that, unlike the case of the Cu-O materials, superconductivity of $LiTi_2O_4$ can be due to an electron-phonon mechanism.

I. INTRODUCTION

The discovery of high-T_c superconductivity in the Cu oxides[1] has increased the interest in studying the original low-T_c superconducting oxide materials. The possibility of having high-T_c superconductivity in transition-metal oxides was opened up by the work of Johnston, Prakash, Zachariasen, and Viswanathan[2] on the spinel system $Li_{1+x}Ti_{2-x}O_4$ phase first obtained by Deschanvres, Raveau, and Sekkal.[3] This system is among the few superconducting spinels (together with[4] $CuRh_2S_4$, CuV_2S_4, and $CuRh_2Se_4$), has the highest observed T_c (11 K),[5,6] and is the only superconducting spinel oxide.[5] In fact, very few oxide spinel compounds show metallic behavior. $Li_{1+x}Ti_{2-x}O_4$ shows a homogeneity range for $0<x<\frac{1}{3}$. The superconducting properties tend to disappear for high x values[5,6] ($x \gtrsim 0.15$) and the end member $Li_{4/3}Ti_{5/3}O_4$ shows insulating properties. For $x=0$, Li and Ti occupy the tetrahedral and octahedral sites of a normal spinel structure, respectively; for $x>0$ Li atoms start to randomly occupy octahedral positions.

The crystallographic and chemical properties of $LiTi_2O_4$ present a few interesting points compared with the high T_c Cu-oxide systems: (i) the Ti atoms are in an octahedral coordination with the O atoms, as in the ideal perovskite structure. However, in the high-T_c materials this coordination is either distorted [in $La_{2-x}M_xCuO_4$ (where M represents a divalent alkaline earth metal)] or destroyed by the O vacancies (in $YBa_2Cu_3O_{7-\delta}$, $Bi_2Sr_2CaCu_2O_8$, and $Tl_2Ba_2CaCu_2O_8$) and the local coordination or neighboring octahedra is different from the perovskite structure.[7] (ii) The presence of a mixed "formal" valence $Ti^{3.5+}$ is similar to that, for instance, of $YBa_2Cu_3O_7$ in which a purely ionic picture gives two Cu^{2+} and one Cu^{3+}. However, the position in energy of Ti $3d$ states relative to the O $2p$ states is different from that of Cu $3d$, which implies a different degree of metal-ligand O hybridization.

It is therefore important to understand the properties of $LiTi_2O_4$, and the study of its electronic structure is a necessary step in this direction. Previous electronic structure calculations[8] on spinel systems were focused on the semiconducting sulfide members of this family. Band-structure calculations have just been recently performed for $LiTi_2O_4$ by Satpathy and Martin[9] using the linear-muffin-tin-orbital (LMTO) method.

In this paper,[10] we report results of local-density all-electron full-potential linearized augmented-plane-wave[11] (FLAPW) calculations of the electronic structure of $LiTi_2O_4$ in both its distorted (observed) structure[5,12] —corresponding to a value of the O parameter (see below) $u=0.2626$—and in its ideal ($u=0.25$) structure. The energy bands, density of states, and electronic charge distributions for the states around the Fermi level are presented. Our energy bands are in good agreement with those of Satpathy and Martin for the observed structure and show important changes in the states close to the Fermi level when compared with results for the ideal structure. The possibility of a phononic mechanism for the superconductivity in this material is confirmed by use of the rigid-muffin-tin approximation (RMTA) of Gaspari and Gyorffy[13] to estimate the electron-phonon coupling parameter.

II. STRUCTURE AND METHOD OF CALCULATION

The spinel structure may be viewed as being formed from an ordered arrangement of two different kinds of cubic units. The O atoms have an almost perfect cubic close-packed arrangement and the cations occupy $\frac{1}{8}$ of the tetrahedral sites (Li atoms) and one half of the octahedral sites (Ti atoms). The O positions are not fixed by symmetry but are determined by the internal parameter u which is 0.25 (with the origin fixed at the center of symmetry) in the ideal case. The O atoms form then a perfect fcc sublattice; in the real structure u is 0.2626.[5,12] This represents a shift of the oxygen atoms in a $\langle 111 \rangle$ direction, which enlarges the tetrahedral and compresses the octahedral sites. No symmetry changes are associated with the distortion. The cation ordering gives rise to a trigonal crystal field around the Ti sites. This trigonal component is reduced by the O displacements. In $Li_{1+x}Ti_{2-x}O_4$, the

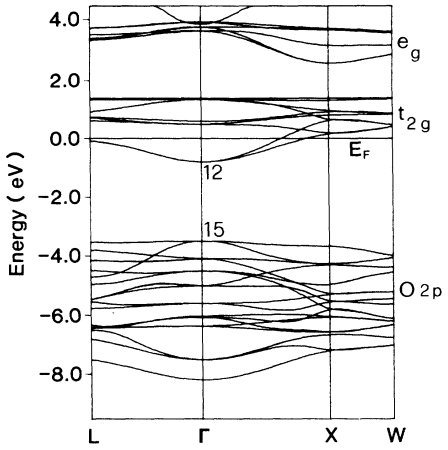

FIG. 1. Energy bands of $LiTi_2O_4$ along the main symmetry lines of the face-centered-cubic Brillouin zone.

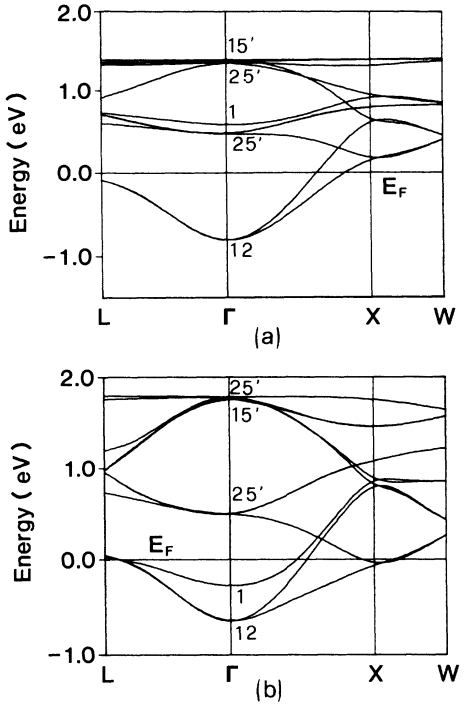

FIG. 2. Energy bands around E_F (t_{2g}) for the (a) observed (distorted) and (b) ideal (undistorted) structure.

tetrahedral sites are still occupied only by Li atoms, while the extra Li_x atoms per formula unit randomly occupy the octahedral positions.[12] The lattice parameter is[6] 8.403 Å for $LiTi_2O_4$ and decreases linearly with x.[2,5,6,12] The unit cell contains two formula units.

The electronic structure of $LiTi_2O_4$ was calculated for the spinel structure using the highly precise FLAPW method[11] with the Hedin-Lundqvist form for the exchange-correlation potential. Inside the muffin-tin spheres, the angular momentum expansion was truncated at $l=8$ for the wave functions and at $l=6$ for the charge density and potential. In the interstitial regions, more than 5800 reciprocal vectors are considered in the Fourier representation of the charge density and potential. The LAPW functions with the wave vector $|\mathbf{k}+\mathbf{G}| \leq K_{\max}$ $=3.5$ a.u. are used in the expansion of the eigenfunctions leading to more than 709 basis functions. (The convergence of the eigenvalues against the changes of $K_{\max}$ was tested with $K_{\max}=3.7$ a.u.; the variation of the eigenvalues was found to be less than 0.04 eV.) Twenty inequivalent sampling k points and the linear tetrahedron scheme are used for the Brillouin zone integration during the self-consistent iterations. The density of states are calculated using 40 k points in the irreducible wedge of the Brillouin zone.

III. RESULTS

A. Energy bands

The energy bands of $LiTi_2O_4$ for the observed structure are shown in Fig. 1. (Not shown are the O 2s bands, which are 1.5 eV wide and whose top is 19.0 eV below E_F.) The main valence band originates mostly from the O 2p states and is 4.70 eV wide. This band is separated by a gap of 2.64 eV from a partially filled conduction band, which contains (for $x=0$) one electron per formula unit and has predominantly Ti 3d character (see below). These results are in good agreement with the photoemission data of Edwards *et al.*,[14] who found an ~5-eV-wide O 2p band separated by a 3 eV gap from the Ti d conduction band. They are also in agreement with the LMTO calculations of Satpathy and Martin,[9] who, however, found a slightly smaller (2.4 eV) gap. Therefore, unlike the high-T_c Cu oxides,[15–18] the metal 3d and O 2p states are clearly separated from one another.

The octahedral crystal-field splits the Ti 3d states into (three) t_{2g} and (two) e_g bands which are nonoverlapping in this compound. (Partially overlapping the e_g band, a band with predominant interstitial character is found at higher energies.) The main bandwidths and energy gaps are given in Table I for both the real and ideal structures, in order to make the differences apparent. The Γ_{15}-Γ_{12} energy gap between the O 2p and Ti 3d t_{2g} states is 0.8 eV lower for the ideal structure. The gap between the t_{2g} and e_g states is also much lower for the ideal structure, as a consequence of the reduced octahedral crystal field. The

TABLE I. Energy gaps and valence (VBW) and conduction (CBW) bandwidths (in eV) in $LiTi_2O_4$ in both the real (distorted) and ideal structures.

	$E_{\Gamma_{15}}-E_{\Gamma_{12}}$	$E_{t_{2g}}-E_{e_g(\Gamma)}$	VBW	t_{2g} CBW	e_g CBW ($\Gamma-X$)
Real	2.68	2.28	4.71	2.19	1.39
Ideal	1.87	1.36	4.41	1.36	1.01

O $2p$ valence bandwidth (VBW) and Ti e_g conduction bandwidth (CBW e_g) are larger in the distorted structure, while the Ti t_{2g} conduction bandwidth (CBW t_{2g}) is smaller. This is consistent with the larger Ti-O hybridization found for the e_g bands, as expected from their different bonding nature, $dp\sigma$ (e_g) versus $dp\pi$ (t_{2g}).

In Fig. 2, we show the energy bands around E_F for both the (a) real and (b) ideal structures. Aside from the different bandwidths, the biggest difference is found in the energy position of the Γ_1 band, which is found slightly above the Γ_{25} band and well above E_F for the real structure while it is partially occupied in the ideal structure. Other minor differences include the position of the Fermi level with respect to the lowest-lying Ti d conduction states at L and X. The different behavior of the Γ_1 band with respect to the oxygen displacement is understood from its strong Ti d–O p hybridization. The charge corresponding to the Γ_1 state of this band has in fact (per unit cell) 18% O p character and 58% Ti d character inside the muffin-tin spheres. As a comparison, the lowest-lying Γ_{12} conduction states are decomposed into 3% O p and 72% Ti d character.[19] The Ti-O hybridization of the Γ_{12} band, however, becomes larger at the zone boundaries, corresponding to higher energies; at X, for instance, very close to the Fermi level, it can be decomposed as having 8.8% O p and 69% Ti d character.

B. Charge density

In order to investigate the nature of the states around E_F, we show in Fig. 3 the charge density corresponding to the lowest-lying Γ_{12} band at Γ and L, plotted in a (001) plane cutting the Ti atoms and (only in the ideal structure) the O atoms and in a (110) plane cutting both Ti and O. At L we observe the presence of a larger Ti-O $dp\pi$ hybridization which, however, is much smaller than that found in the Cu-O high-T_c materials.[15–18] Figure 3 also shows the presence of a Ti-Ti nearest-neighbor interaction. This interaction is, however, reduced by the "out-of-plane" directionality of the Ti t_{2g} orbitals shown in Fig.

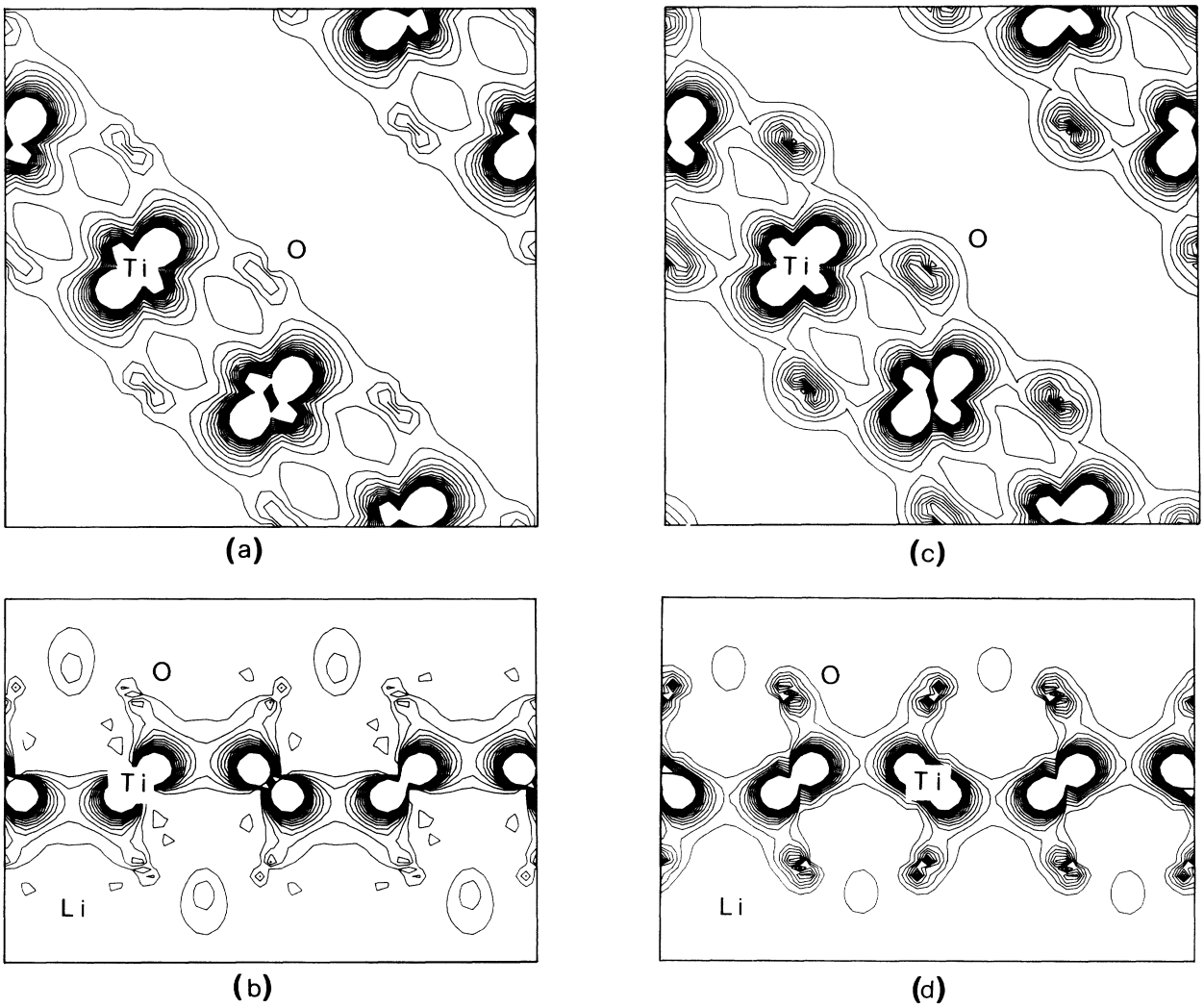

FIG. 3. Charge-density contour plots for the Γ_{12} band [Fig. 2(a)] in the distorted structure at Γ [(a) and (b)] and L [(c) and (d)], in a (001) plane cutting the Ti atoms [(a) and (c)] and in a (110) plane [(b) and (d)]. Contours are given on a linear scale and successive contours are separated by $0.4\times10^{-3}\ e/a_0^3$.

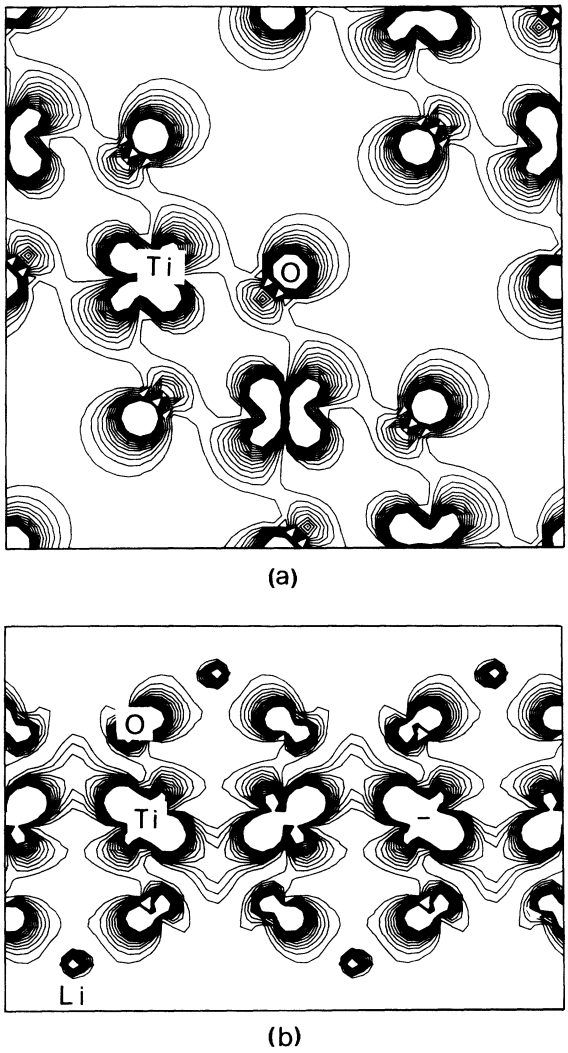

FIG. 4. Charge-density contour plots for the Γ_1 state in the distorted structure. Planes and contours as in Fig. 3.

3. Figure 4 shows the charge-density contour plots of the Γ_1 state. The large Ti-O hybridization is apparent, and accounts for its high sensitivity to the O displacements.

C. Density of states

Figures 5 and 6 show the densities of states of $LiTi_2O_4$ in the distorted and ideal structures, respectively. The density of states (DOS) at the Fermi level $N(E_F)$ is largely reduced by the O displacements, being 3.2 states/eV formula unit in the real case and 5.9 states/eV formula unit in the ideal case. The lowering of $N(E_F)$ associated with the O displacements is consistent with the observed stability of the distorted structure relative to the ideal one. If one identifies a high $N(E_F)$ with a potential instability in the usual way, then one may understand the distortion as being electronically driven. [It should be remembered, however, that similar distortions also occur[8] in the semiconducting spinels, in which such arguments about high $N(E_F)$ values do not apply.] The value of $N(E_F)$ for the

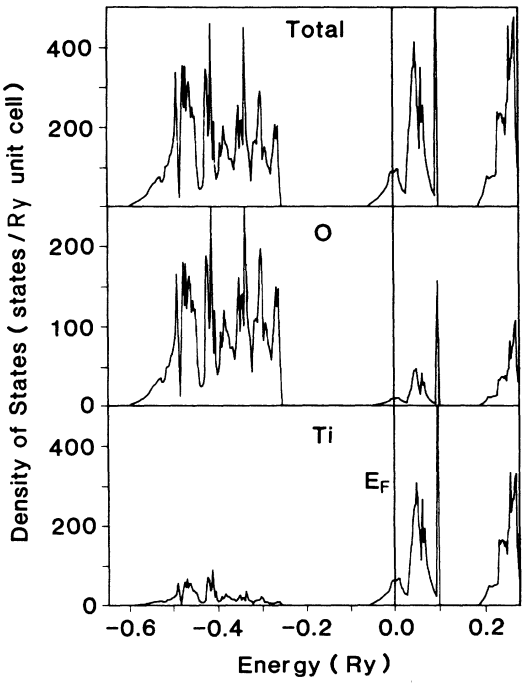

FIG. 5. Total and projected DOS for the observed (distorted) structure.

real structure is in good agreement with that obtained by Satpathy and Martin (3.3 states/eV formula unit).

Experimental estimates of the density of states at E_F can be obtained from magnetic susceptibility measurements[5] and from low-temperature specific-heat experiments.[20] The value obtained by Johnston from the mea-

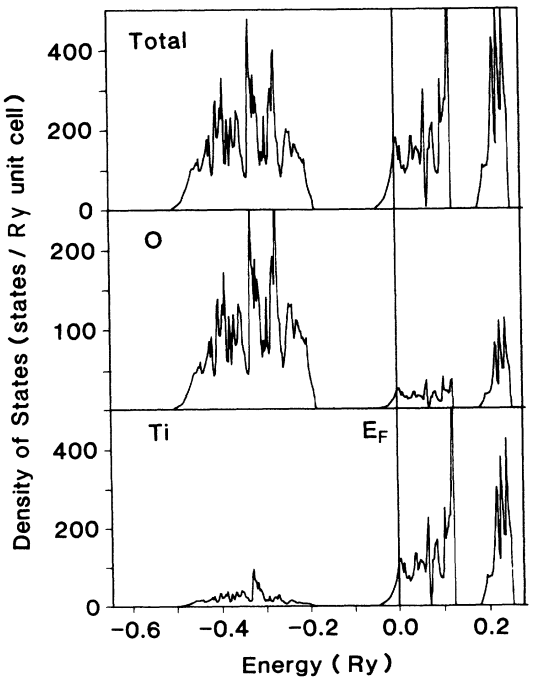

FIG. 6. Total and projected DOS for the ideal (undistorted) structure.

sured magnetic susceptibility[5] is $N^{\chi}(E_F)$=6.8 states/eV-formula unit. Comparison of this value with our calculated $N(E_F)$ value gives an exchange enhancement factor of 2.1. We have calculated the Stoner factor[21] $S=N(E_F)I$ to be $\sim$0.45; the corresponding enhancement factor $(1-S)^{-1}$ (i.e., 1.8) is seen to be consistent with the above estimate.

From a comparison of the calculated value of $N(E_F)$ and the experimental specific-heat value, $N^{\gamma}(E_F)$, one can get information about the enhancement factor λ_{tot} defined as $N^{\gamma}(E_F)=N(E_F)(1+\lambda_{tot})$ where $\lambda_{tot}=\lambda_{e\text{-ph}}+\lambda_{e\text{-}e}+\lambda_{SF}$ is written in terms of electron-phonon, electron-electron, and spin-fluctuation contributions. Using the measured specific-heat data given by McCallum *et al.*[20]—which yields a measured $N^{\gamma}(E_F)$=9.1 states/eV-formula unit—we estimate λ_{tot} to be 1.8.

The atomic projected partial densities of states (PDOS) at E_F in the distorted structure show that the states at E_F are largely due to Ti 3*d* states (71%), with about a 9% contribution from O 2*p* states and about an 18% interstitial contribution. In the ideal structure, Ti *d* contributes 66% of the total $N(E_F)$ value, while the contribution of the O *p* states increases to 14% and the interstitial contribution to 19%. The (relative) increased O contribution is consistent with the lowering in energy of the highly O-hybridized Γ_1 band at around E_F. The shortening of the Ti-O distance in the real structure raises, in fact, the energy of this antibonding band and leads to a smaller $N(E_F)$ value and, as stated above, to greater stability. The partial DOS's in Fig. 5 show that the O contribution is larger in the upper part than in the lower of the t_{2g} conduction band. This is in agreement with the photoemission data of Edwards *et al.*[14]

If we now compare the $N(E_F)$ (per metal atom) in $LiTi_2O_4$ and in the Cu-O high-T_c materials, we find the following results: in $LiTi_2O_4$ we have 1.58 states/(eV Ti atom), while in $YBa_2Cu_3O_{7-\delta}$ we have[16] 1.13 states/(eV Cu atom) for δ=0; in $La_{2-x}Sr_xCuO_4$ we have[15] 1.2 and 1.9 states/(eV Cu atom) for x=0 and 0.16, respectively. Therefore $N(E_F)$ per Ti atom in $LiTi_2O_4$ is higher than in $YBa_2Cu_3O_{7-\delta}$ per Cu atom but it is comparable with that of the $La_{2-x}Sr_xCuO_4$ system (again per Cu atom).

The angular momentum decomposed total valence charges inside the muffin-tin spheres are listed in Table II.

TABLE II. *l*-decomposition of the total valence charge inside the muffin-tin spheres given in terms of electrons per atom: (a) real (observed) structure, (b) ideal (undistorted) structure. The muffin-tin radii are 1.6, 2.15, and 1.565 a.u., respectively, for Li, Ti, and O.

	s	*p*	*d*	Total
		(a) Observed structure		
Li	0.03	0.07	0.01	0.11
Ti	0.15	0.27	1.61	2.12
O	1.55	3.48	0.01	5.04
		(b) Ideal structure		
Li	0.05	0.12	0.02	0.20
Ti	0.14	0.22	1.54	1.94
O	1.56	3.41	0.01	4.97

TABLE III. The McMillan-Hopfield parameter η per atom (eV/Å^2) for each structure of the bimolecular $(LiTi_2O_4)_2$ unit cell.

	Real	Ideal
η[Li]	0.000	0.027
η[Ti]	0.498	0.498
η[O]	0.283	0.491

Each Ti sphere is seen to contain 1.61 *d*-like electrons in the real structure and is somewhat larger (by 0.07*e*) than in the ideal structure. Also, the O atomic spheres have somewhat more charge (again, 0.07*e*) in the real structure, with a net displacement of charge from the interstitial to inside the sphere regions; note also the larger charge inside the Li spheres for the ideal structure. Both observations can be correlated to the shorter Li-O distance in the ideal case. The shorter distance implies, in fact, higher Li-O hybridization, and therefore a higher Li content in the O valence band.

D. Electron-phonon interaction

To investigate the origin of superconductivity in $LiTi_2O_4$, we have calculated the Hopfield-McMillan parameter η by using the crude RMTA of Gaspari and Gyorffy.[13] The calculated η values are listed in the Table III. Similar to the PDOS results, the dominant contributions to η come mostly from O and Ti ions. However, while the contribution of the O atoms to $N(E_F)$ is much smaller than that from Ti atoms, the η(O,total)=2.264 (vs 3.928) value is significantly larger than the η(Ti,total)=1.992 (vs 1.992) for the real (vs ideal) structure (these values refer to the unit cell, i.e., 2 formula units). In view of the lighter O mass (cf. below), this fact indicates the greater importance of O ions relative to Ti ions in the electron-phonon interaction and, hence, in their potential contribution to superconductivity. At the minimum, these results emphasize the importance of the Ti*d*-O*p* interaction. The Li ions have negligibly small η

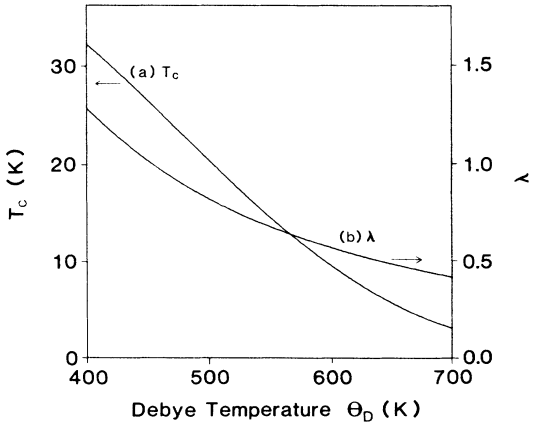

FIG. 7. T_c and λ as obtained from the McMillan equation and from our rigid-ion calculations (see text).

values within the RMTA, especially for the real spinel structure.

The electron-phonon coupling strength λ can be factorized as[22]

$$\lambda=\sum_j \lambda_j, \quad \lambda_j=\frac{\eta_j}{M_j\langle\omega^2\rangle}, \tag{1}$$

where λ_j is the decomposition of λ for each atom j; M_j, their masses; and $\langle\omega^2\rangle$ can be crudely taken as $\langle\omega^2\rangle=\frac{1}{2}\Theta_D^2$ (Θ_D is the Debye temperature). Based upon the assumptions that only the electron-phonon interactions contribute to the superconductivity and that the effective Coulomb pseudopotential $\mu^*=0.1$, we can use the calculated η values to estimate the superconducting transition temperature T_c by using McMillan's formula

$$T_c=\frac{\Theta_D}{1.45}\exp\left[-\frac{1.04(1+\lambda)}{\lambda-\mu^*(1+0.62\lambda)}\right]. \tag{2}$$

The variable range of λ and T_c as a function of Θ_D is shown in Fig. 7. The observed value of $T_c=12$ K of $LiTi_2O_4$ corresponds to the rms phonon frequency or Debye temperature $\Theta_D=575$ K and the electron-phonon coupling strength λ of about 0.6. These values of λ and Θ_D fall into the range suggested by McCallum *et al.*[20] [namely, $\lambda=0.58$ with $\Theta_D=685$ K and $\mu^*=0.1$ in Eq. (2)]. This estimate (even though very crude) indicates that the superconducting critical temperature $T_c\simeq 12$ K of $LiTi_2O_4$ can be understood within BCS theory based upon the electron-phonon interaction. We note, however, that the value of $\lambda_{tot}=1.8$ derived previously from the specific-heat data is much larger than the $\lambda_{e\text{-ph}}$ calculated value (~ 0.6). Since the Stoner enhancement factor is ~ 2, it is unlikely that this large difference between the estimates could be due to spin-fluctuation effects. Hence its origin needs further study.

ACKNOWLEDGMENTS

This work was supported by the National Science Foundation (Grant No. DMR85-20280 through the Northwestern University Materials Research Center) and by a computing grant from its Division of Advanced Scientific Computing at the National Center for Supercomputing Applications, University of Illinois, Champaign-Urbana, and at the Air Force Weapons Laboratory, Kirkland, AFB.

[1] J. G. Bednorz and K. A. Müller, Z. Phys. B **64**, 189 (1986); M. K. Wu *et al.*, Phys. Rev. Lett. **58**, 908 (1987); H. Maeda, Y. Tanaka, M. Fukutomi, and T. Asano, Jpn. J. Appl. Phys. **27**, L209 (1988); C. W. Chu, J. Bechtold, L. Gao, P. H. Hor, Z. J. Huang, A. L. Meng, Y. Y. Sun, Y. Q. Wang, and Y. Y. Ywe, Phys. Rev. Lett. **60**, 941 (1988); Z. Z. Sheng, A. M. Hermann, E. El Ali, C. Almason, J. Estrada, T. Datta, and R. J. Matson, *ibid.* **60**, 397 (1988).

[2] D. C. Johnston, H. Prakash, W. H. Zahariasen, and R. Viswanathan, Mater. Res. Bull. **8**, 777 (1973).

[3] A. Deschanvers, B. Raveau, and Z. Sekkal, Mater. Res. Bull. **6**, 699 (1971).

[4] N. H. Van Maaren, G. M. Schaeffer, and F. K. Lotgering, Phys. Lett. **25A**, 238 (1967); M. Robbins, R. H. Willens, and R. C. Miller, Solid State Commun. **5**, 933 (1967); R. N. Shelton, D. C. Johnson, and H. Adrian, *ibid.* **20**, 1077 (1976).

[5] D. C. Johnston, J. Low Temp. Phys. **25**, 145 (1976).

[6] M. R. Harrison, P. P. Edwards, and J. B. Goodenough, Philos. Mag. B **52**, 679 (1985).

[7] F. S. Galasso, *Structure and Properties of Inorganic Solids* (Pergamon, Oxford, 1970).

[8] See, for instance, A. Baldereschi, F. Meloni, F. Aymerich, and G. Mula, in *Ternary Compounds,* edited by G. D. Holah, Institute of Physics Conference Series No. 35 (IOP, Bristol, 1977), p. 193, and references therein.

[9] S. Satpathy and R. M. Martin, Phys. Rev. B **36**, 7269 (1987).

[10] Results were first presented by A. J. Freeman, S. Massidda, and J. Yu, Bull. Am. Phys. Soc. **33**, 608 (1988).

[11] H. J. F. Jansen and A. J. Freeman, Phys. Rev. B **30**, 551 (1984).

[12] R. J. Cava, D. W. Murphy, S. Zahuzak, A. Santoro, and R. S. Roth, J. Solid State Chem. **53**, 64 (1984).

[13] G. D. Gaspari and B. L. Gyorffy, Phys. Rev. Lett. **28**, 801 (1972).

[14] P. P. Edwards, E. G. Egdell, I. Fragala, J. B. Goodenough, M. R. Harrison, A. F. Orchard, and E. G. Scott, J. Solid State Chem. **54**, 127 (1984).

[15] J. Yu, A. J. Freeman, and J.-H. Xu, Phys. Rev. Lett. **58**, 1035 (1987); L. F. Mattheis, *ibid.* **58**, 1028 (1987).

[16] S. Massidda, J. Yu, A. J. Freeman, and D. D. Koelling, Phys. Lett. A **122**, 198 (1987); J. Yu, S. Massidda, A. J. Freeman, and D. D. Koelling, *ibid.* **122**, 203 (1987).

[17] S. Massidda, J. Yu, and A. J. Freeman, Physica C **152**, 251 (1988); M. S. Hybertsen and L. F. Mattheis, Phys. Rev. Lett. **60**, 1661 (1988); H. Krakauer and W. E. Pickett, *ibid.* **60**, 1665 (1988).

[18] J. Yu, S. Massidda, and A. J. Freeman, Physica C **152**, 273 (1988).

[19] Due to the different sphere radii used in the two calculations, this value should not be compared with that given in Ref. 7 (71% Ti *d* and 10% O *p*).

[20] R. W. McCallum, D. C. Johnston, C. A. Luengo, and M. B. Maple, J. Low Temp. Phys. **25**, 177 (1976).

[21] T. Jarlborg and A. J. Freeman, Phys. Rev. B **22**, 2332 (1980).

[22] B. M. Klein and W. E. Pickett, in *Superconductivity in d- and f-band Metals,* edited by W. Buckel and W. Weber (Kernforschungszentrum, Karlsruhe, 1982).